

Properties of CdZnTe detectors in the Burst Alert Telescope (BAT) Array

Goro Sato^{acde}, Tadayuki Takahashi^a, Kazuhiro Nakazawa^a, Shin Watanabe^{ac}, Makoto Tashiro^b, Masaya Suzuki^b, Yuu Okada^c, Hiromitsu Takahashi^c, Ann Parsons^d, Jack Tueller^d, Hans Krimm^d, Scott Barthelmy^d, Jay Cummings^{de}, Craig Markwardt^{df}, Derek Hullinger^{df}, Neil Gehrels^d, Ed Fenimore^g, David Palmer^g, Tony Dean^h, and Dave Willis^h

^aInstitute of Space and Astronautical Science (ISAS), 3-1-1 Yoshinodai, Sagamihara, Kanagawa, 229-8510, Japan

^bUniversity of Saitama, Japan

^cUniversity of Tokyo, Japan

^dNASA/Goddard Space Flight Center, USA

^eUniversities Space Research Association, USA

^fUniversity of Maryland, USA

^gLos Alamos National Laboratory, USA

^hUniversity of Southampton, UK

ABSTRACT

The properties of 32k CdZnTe detectors have been studied in the pre-flight calibration of Burst Alert Telescope (BAT) on-board the Swift Gamma-ray Burst Explorer (scheduled for launch in January 2004). After corrections of the linearity and the gain, the energy resolution of summed spectrum is 7.0 keV (FWHM) at 122 keV. In order to construct response matrices for the BAT instrument, we extracted mobility-lifetime ($\mu\tau$) products for electrons and holes in the CdZnTe. Based on a new method applied to ⁵⁷Co spectra taken at different bias voltages, $\mu\tau$ for electrons ranges from 5.0×10^{-4} to 1.0×10^{-2} cm²V⁻¹, while $\mu\tau$ for holes ranges from 1.0×10^{-5} to 1.7×10^{-4} cm²V⁻¹. We show that the distortion of the spectrum and the peak efficiency of the BAT instrument are well reproduced by the $\mu\tau$ database constructed in the calibration.

Keywords: CdZnTe, mobility, lifetime, $\mu\tau$ products, Swift, BAT

1. INTRODUCTION

Cadmium Telluride (CdTe) and Cadmium Zinc Telluride (CdZnTe, CZT) semiconductor materials have attracted the most attention as X-ray and gamma-ray detectors among the semiconductor materials with a wide band gap. Recently, several astronomical missions have been designed based on CdTe or CdZnTe. Their good energy resolution and the ability to fabricate compact arrays are very attractive features in comparison with inorganic scintillation detectors coupled to either photodiodes or photo-multiplier tubes. International Gamma Ray Astrophysics Laboratory (INTEGRAL) satellite and Swift Gamma-ray Burst Explorer are the first missions that make use of a large number of CdTe or CdZnTe detectors for the spectroscopy and the imaging in the energy band from several 10 keV to several hundred keV. The ISGRI is one of three instruments on board the INTEGRAL mission. It uses 16,384 planar CdTe ($4 \times 4 \times$ mm² large, 2 mm thick) detectors. The Burst Alert Telescope (BAT) on board the Swift satellite is an assembly of 32,768 planar CdZnTe detectors ($4 \times 4 \times$ mm² large, 2 mm thick) to form a 1.2 m \times 0.6 m sensitive area. Both instruments are designed as coded mask aperture imaging telescopes with a wide field-of view (FOV), which provides imaging capability and spectroscopy.

Further author information: (Send correspondence to G.S.)

G.S.: E-mail: gsato@astro.isas.ac.jp, Telephone: +81-42-759-8545

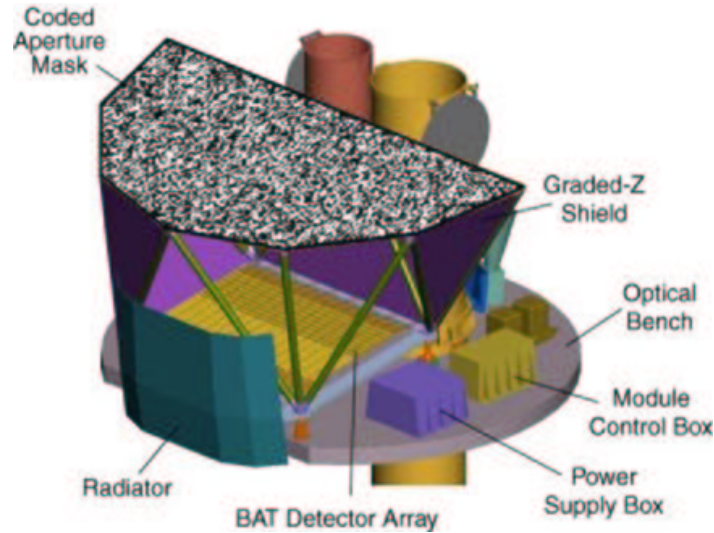


Figure 1. Cut away drawing of BAT instrument, which has a 3 m^2 of D-shaped coded aperture mask with 5 mm pixels. The CdZnTe array is 5200 cm^2 with 4mm detectors. Graded-Z shielding reduces the background due to cosmic diffuse emission.

Despite the recent advances, it is still worth pointing out that the considerable amount of charge loss in CdTe and CdZnTe limits their capability as high resolution spectrometers. This is due mainly to the poor charge transport properties, especially for holes. Due to the low mobility and the short lifetime of the carriers, the electron and hole pairs generated by gamma-ray irradiation cannot be fully collected, and as a result, a broad low energy tail is seen in the detector's energy spectrum. Though the charge transport properties of carriers have been investigated by various authors, the number of samples were always limited. Since the BAT instrument is made of 32,768 CdZnTe detectors from a number of ingots, the pre-flight calibration provides us a unique opportunity to study the distribution of parameters.

In this paper, first, we review of the BAT instrument, and describe pre-flight calibration. Then, we report the results of $\mu\tau$ products extraction from 32K individual CdZnTe detectors. Finally, we show how to utilize these parameters in a Monte Carlo simulation.

2. THE BURST ALERT TELESCOPE

The Burst Alert Telescope (BAT) is a highly sensitive, large FOV instrument designed to provide critical GRB triggers and 4-arcmin positions. It is a coded aperture imaging instrument with a 1.4 steradian field-of-view (half coded). The energy range is 15-150 keV for imaging with a non-coded response up to 500 keV (Gehrels et al. 2003). BAT is anticipated to detect and locate hundreds of bursts per year to better than 4 arc minutes accuracy. Using this prompt burst location information, Swift can slew quickly to point x-ray and optical telescopes at the burst.

The basic numbers describing the BAT instrument are listed in Table 1. The BAT has a large (5243 cm^2) hard X-ray detector plane and an even larger (3.2 m^2) coded aperture mask located 1 m above the detector plane. There are 32,768 pieces of $4 \text{ mm} \times 4 \text{ mm} \times 2 \text{ mm}$ CdZnTe (CZT) detector elements in the BAT. Groups of 128 detector elements are assembled into 8×16 arrays. Detector modules, each containing two such arrays, are further grouped by eights into blocks. In the module, the signals from each of the 128 detectors are read out by a single XA1 Application Specific Integrated Circuit (ASIC) which contains 128 individual signal processing chains. This 128-channel XA1 readout chip was designed and produced by Integrated Detector and Electronics of Norway.

The BAT mask is constructed using $5 \text{ mm} \times 5 \text{ mm} \times 1 \text{ mm}$ lead plates attached to a self-supporting 0.4 g/cm^2 substrate fabricated from Korex fiber honeycomb materials. With 4 mm square focal plane detector elements and 5 mm square mask pixels, BAT will have angular resolution better than 22 arc minutes and will determine GRB source

locations to ~ 4 arc minutes for bursts detected at 5 sigma or brighter. Graded-Z shielding is attached to the sides of the BAT structure to significantly reduce background from gamma rays coming from outside the aperture (shown in Fig. 1).

Table 1. BAT instrument properties

Telescope Property	Description
Aperture	Coded mask
Detecting Area	5200 cm ²
Detector	CdZnTe
Detector Operation	Photon counting
Field of View	1.4 sr (partially-coded)
Detection Elements	256 modules of 128 elements
Detector Size	4 mm \times 4 mm \times 2 mm
Telescope PSF	20 arcmin
Energy Range	15-150 keV

The CdZnTe array will have a nominal operating temperature of 20 degrees and its thermal gradients (temporal and spatial) will be kept to within ± 1 degree. The typical bias voltage is -200 V, with a maximum of -300 V. The CdZnTe material used in the BAT is manufactured by eV Products using the High Pressure Bridgman (HPB) technique. The low leakage current due to the high resistivity of HPB-grown CdZnTe and its good electron transport is expected to result in good spectral performance. Nevertheless, there are a few drawbacks associated with this new detector material. Although the ingots are of very large volume, the present HPB technique yields only polycrystals with a non-uniform distribution of $\mu\tau$ products (e.g. Takahashi and Watanabe, 2001¹).

3. BAT PRE-FLIGHT CALIBRATION

In order to understand the BAT instrument's response to incident 15-150 keV gamma-rays, the intensive pre-flight calibration was performed immediately after the modules are constructed. The calibration is divided into two phases; one is for each block individually and the other is for the entire instrument in the big clean room at NASA/Goddard Space Flight Center (Parsons et al. 2003²).

The main objective of the first block-level test is to evaluate key mobility and lifetime parameters for each detector element. For this, we have acquired spectra of various radioactive sources such as ²⁴¹Am, ⁵⁷Co, ¹⁰⁹Cd and ¹³⁷Cs at different bias voltages, different temperatures and different incident angles. Then we analyzed the resulting shift of the photopeak position and the change in the amount of tail in the spectra. In order to minimize the scattering component in the spectra, the measurements were performed in such a way that the radioactive source is mounted inside a box made of lead with a FOV that is sufficient to irradiate all 2048 CdZnTe detectors in the block. A large shielding plate was attached to the box to prevent a spectrum component coming from scattering off the room's ceiling.

After we finished the block-level test, we mounted the block in the BAT array. In the end, all sixteen blocks are installed on the detector array plate which is located 1 meter under the coded aperture mask. In the calibration with this set up, the detector signals are modulated by the mask pattern. A radioactive source was set on a slide table held 2 m above the mask. Fig. 2 demonstrates the imaging capability of the BAT. We moved the source such that the trajectory follows the characters "BAT". After the de-convolving the image using an FFT image reconstruction software, we can clearly see the pattern. The angular resolution of 23.7 arcmin (FWHM) is obtained from the point source observation.

The spectrum of the entire detector plane is constructed correcting for the linearity and the gain of the readout electronics and the shift of the photopeak due to the variation of the charge transport properties (see the next section).

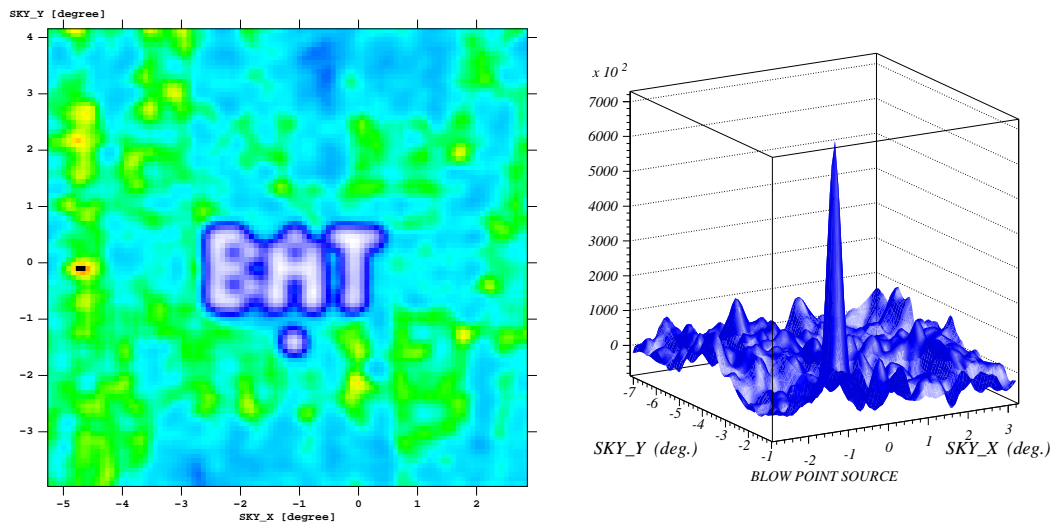


Figure 2. Reconstructed images, taken by irradiating with gamma-rays from a ^{57}Co radioactive source onto the BAT detector plane through the coded mask in a pre-flight ground calibration test. The count rates in the individual detectors are processed using FFT image reconstruction software. The right figure is an enlarged image of a point source, which is resolved with 23.7 arc minutes of PSF(FWHM).

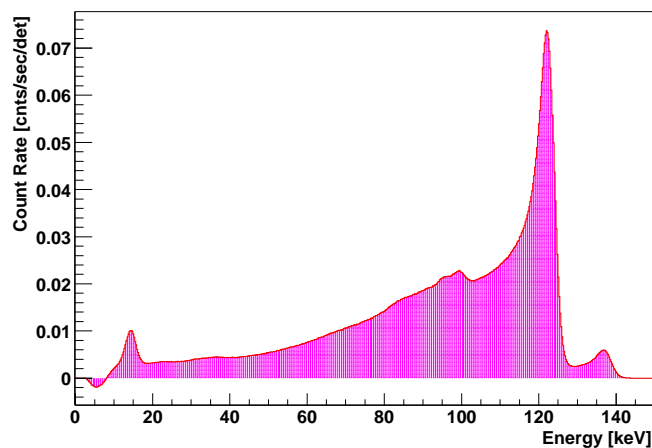


Figure 3. Summed spectrum of 32K CdZnTe detectors (the entire BAT array) for ^{57}Co . The 14, 122 and 136 keV lines are clearly seen. The composite FWHM of the 122 keV lines is 7.0 keV

To obtain the summed spectra, we also need to apply the mask weighting method. Events recorded by the detectors that are completely unshadowed (i.e., no mask tiles lie between the detector and the source) are given a mask weight of +1. Events recorded by detectors that are completely shadowed by the mask (i.e., the detector is entirely shielded from the source by one or more mask tiles) are given a mask weight of -1. Detectors that are partially shadowed by the mask are given mask weights that lie somewhere between +1 and -1, depending on the fraction of the detector that lies in shadow. As shown in Fig. 3, in the processed spectrum, the 14, 122 and 136 keV lines are clearly seen. The energy resolution of the summed spectrum for the 122 keV lines is 7.0 keV (FWHM).

Table 2. Parameters for the fitting model function

parameter	Description
E_γ	energy of incident γ -ray
$(\mu\tau)_e$	$\mu\tau$ product of electron
$(\mu\tau)_h$	$\mu\tau$ product of hole
E	strength of electric field
σ	resolution excluding the tail structure
CH_{\max}	channel where Hecht equation becomes unity

4. CHARACTERIZATION OF 32K CDZnTE DETECTORS

To evaluate the key mobility and lifetime parameters for each detector, we calculate a spectral fitting function which takes the charge transport properties and the interaction position distribution into account. Assuming a constant electric field throughout the detector volume, the charge transport efficiency is described as a function of the interaction depth from the cathode surface for a specific set of $\mu\tau$ products (Hecht equation).³ In order to obtain the depth distribution accurately, we performed a Monte Carlo simulation, which tracks the photons fluorescence (23 keV for Cd and 27 keV for Te), which could escape from the detector, especially when the emission takes place very close to the cathode surface. The detector response for monochromatic γ -rays is generated by calculating the relative pulse height from the Hecht equation at each depth and integrating them up from cathode to anode by following the depth distribution as a weight. The resultant spectrum gives the shape predicted from the parameters listed in Table 2. While the $\mu\tau$ electron mainly changes the peak position, the $\mu\tau$ hole affects the amount of low energy tail. This therefore allows us to extract the $\mu\tau$ products from the individual detectors (see Sato et. al, 2002⁴).

We have acquired ⁵⁷Co spectra at three different bias voltages (100, 150, 200 V) at the temperature of 20°C and have applied the spectral fitting method to 122 keV peaks for 28672/32768 CdZnTe detectors, so far, and the left is still to be determined. The fitted region includes the 136 keV line and is restricted to above 107 keV to exclude the escape peaks. We successfully extracted 26581 ($\sim 92\%$) sets of $\mu\tau$ for electron ranging from 5.0×10^{-4} to 1.0×10^{-2} cm²V⁻¹, and $\mu\tau$ for hole ranging from 1.0×10^{-5} to 1.7×10^{-4} cm²V⁻¹. Fig. 4, a color map for $\mu\tau$ electron shows patches of detector groups classified by the $\mu\tau$ electron values. We investigated this geometrical structure and found that this perfectly corresponds to the manufacturing lot difference of crystal ingot. In the color map of $\mu\tau$ holes shown in Fig. 5, the geometrical structure can be seen as well as for $\mu\tau$ electrons but more randomly distributed even in the group of detectors originating from the same ingot. Fig. 6 is a cross plot of $\mu\tau$ electron and $\mu\tau$ hole, showing a slight correlation. The majority of detectors (57%) are found in the region where $\mu\tau$ electron is more than 3.0×10^{-3} cm²V⁻¹ and $\mu\tau$ hole is more than 4.0×10^{-3} cm²V⁻¹.

5. DEVELOPMENT OF THE BAT DETECTOR SIMULATOR

In order to study the response of the BAT instrument when installed in the Swift spacecraft, it is important that the simulation program takes all the satellite structure into account, because the scattering the material in the satellite contributes significantly to the energy spectrum. Also, the activation due to the particle interaction is another important issue to cope with. For this, we have developed a simulation program, called Sim-SwiMM. In the Sim-SwiMM, every detail of the materials in the instruments and the entire Swift satellite are included as a mass model under the framework of Geant 4.⁵ Since secondary generated γ -rays can be traced by Geant4, the escapes are treated properly.

In the simulation, we take the measured $\mu\tau$ products from the database corresponding to the interacted pixel and apply the Hecht equation to the energy measured. With the mask weighting method, the simulated data are summed up in the same manner as the calibration data and smoothed with the statistical noise and the averaged electronics noise in the calibration. The simulated spectrum agrees well with the actual data, as shown in Fig. 7. To investigate the discrepancy in the low energy region and 14 keV peak, some more passive materials should be included in the simulation geometry. This result however proves that we can predict and reproduce various responses of the detector based on the measured $\mu\tau$ products for each detector.

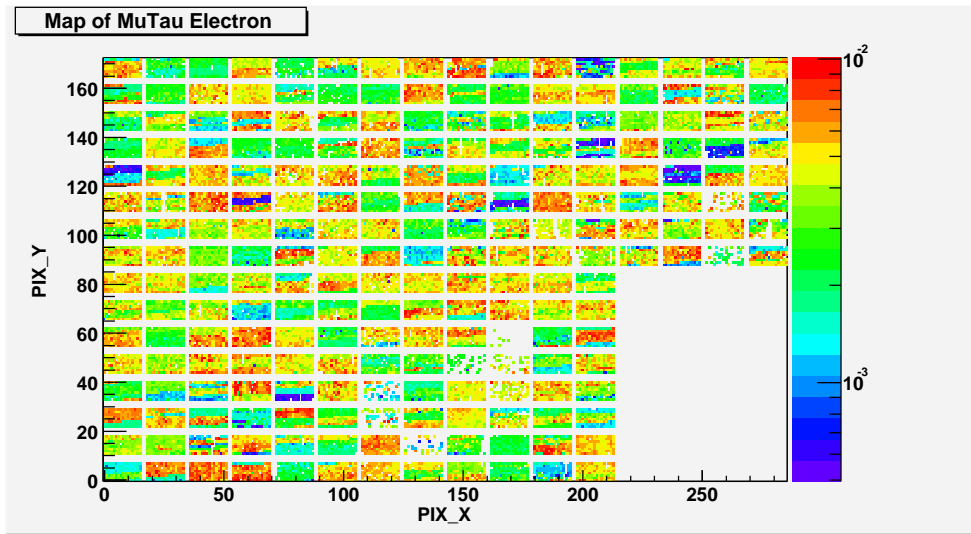


Figure 4. A color map for $\mu\tau$ electrons determined by spectral fitting in 256×128 (32768) pixels with some gaps between each module 128-detector module. 99 % of the $\mu\tau$ values for electrons ranges from 5×10^{-4} to $1 \times 10^{-2} \text{ cm}^2\text{V}^{-1}$. The large geometrical structures are found to correspond to the different originated ingots. The blanks of 16 modules remaining at bottom the right are still to be determined.

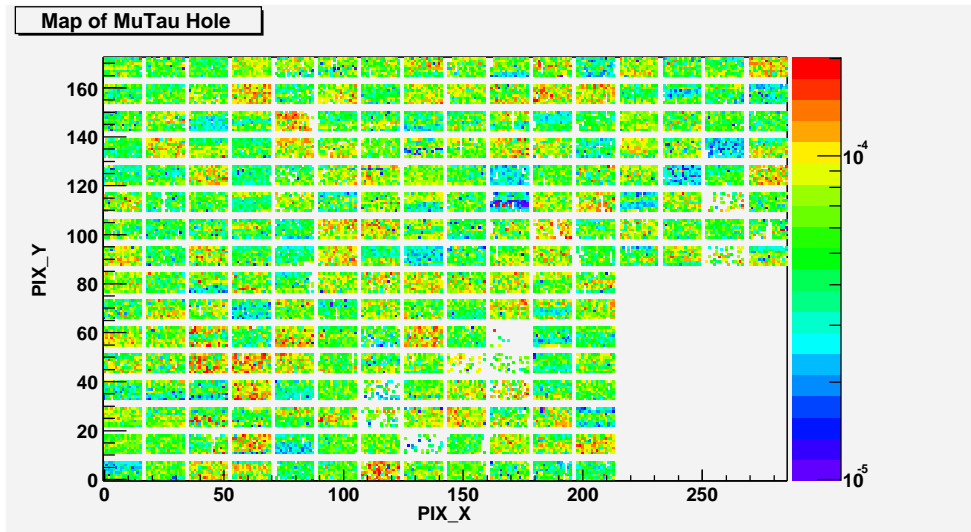


Figure 5. A color map for $\mu\tau$ holes determined by spectral fitting in 256×128 (32768) pixels with some gaps between each 128-detector module. 99 % of the $\mu\tau$ values for holes range from 1.0×10^{-5} to $1.7 \times 10^{-4} \text{ cm}^2\text{V}^{-1}$. The large geometrical structures can be seen as well as $\mu\tau$ electrons but are more randomly distributed even in groups of detectors originating from the same ingot. The blanks of 16 modules remaining at the bottom right are still to be determined.

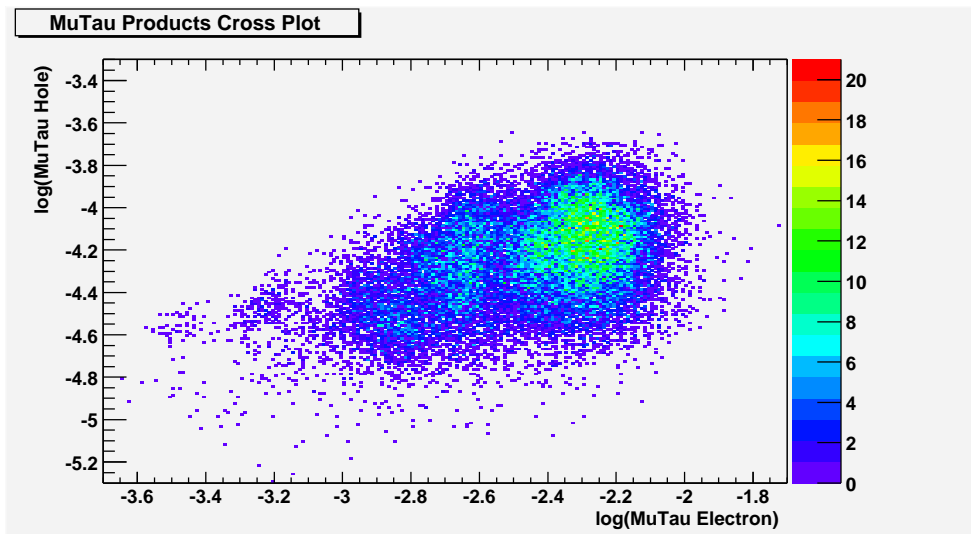


Figure 6. A cross plot of $\mu\tau$ electron and $\mu\tau$ hole. These parameters are slightly correlated. The majority of detectors (57 %) are found in the region where $\mu\tau$ electron is more than $3.0 \times 10^{-3} \text{ cm}^2\text{V}^{-1}$ and $\mu\tau$ hole is more than $4.0 \times 10^{-3} \text{ cm}^2\text{V}^{-1}$

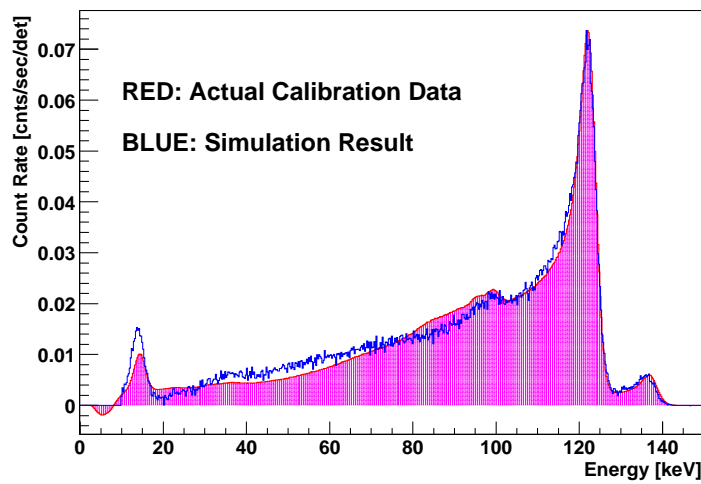


Figure 7. Simulated summed spectrum of 32K CdZnTe detectors (the entire BAT array) for ^{57}Co (blue) overlaid on the actual calibration data (red). The measured $\mu\tau$ products are applied to individual detectors each with different values. The simulation data is normalized to the 122 keV photopeak and smeared with the electronics noise of 1.4 keV and statistical noise.

6. SUMMARY

The energy response of 32K CdZnTe detectors is studied in the pre-flight calibration of the Burst Alert Telescope (BAT) on board the Swift Gamma-ray Burst Explorer (scheduled for launch in January 2004). The dimensions of each individual, planar CdZnTe detector are 4 mm×4 mm×2 mm. Due to the low mobility and the short lifetime of the carriers, the electron and hole pairs generated by gamma-ray irradiation cannot be fully collected, and as a result, a broad low energy tail is seen in the detector's energy spectrum. To evaluate these key mobility and lifetime parameters for each detector, we have acquired ^{57}Co spectra at three different bias voltages and observed the resulting shift of the peak position and the change of the amount of tail at these different bias voltages. We simultaneously fit the three spectra to a model that takes the charge transport properties and the interaction position distribution into account. This allows us to extract the mobility-lifetime products for the individual detectors and to reveal that there exists variations in these parameters of over 1 order of magnitude. We have developed a simulation program of the BAT instrument which takes all the satellite structures into account. This program, Sim-Swimm, reads $\mu\tau$ parameters from the database we have constructed, and simulates the detailed response of the CdZnTe detectors to gamma-rays and particles. With this program, we can study the spectral and imaging response of the BAT instrument and estimate the actual Swift sensitivity in flight.

REFERENCES

1. T. Takahashi and S. Watanabe, "Recent progress in cdte and cdznte detector," *IEEE Trans. Nucl. Sci.* **48**, 2001.
2. A. Parsons, "Swift/BAT calibration and the estimated bat hard x-ray survey sensitivity," *Proc. SPIE in press*, 2003.
3. K. Hecht, "Zum mechanismus des lichtelektrischen primastromes in isolierenden kristallen," *Zeits. Phys.* **77**, p. 235, 1932.
4. G. Sato, T. Takahashi, M. Sugiho, M. Kouda, S. Watanabe, Y. Okada, T. Mitani, and K. Nakazawa, "Characterization of cdte/cdznte detectors," *IEEE Trans. Nucl. Sci.* **49**, pp. 1258–1263, 2002.
5. *Geant4*. <http://wwwinfo.cern.ch/asd/geant4/geant4.html>.